

## A Note on the Stability Indicator of the Atlantic Meridional Overturning Circulation

WEI LIU

*Center for Climatic Research, University of Wisconsin—Madison, Madison, Wisconsin*

ZHENGYU LIU

*Key Laboratory of Meteorological Disaster of Ministry of Education, School of Marine Sciences, Nanjing University of Information Science and Technology, Nanjing, and Laboratory for Climate, Ocean and Atmosphere Studies, Peking University, Beijing, China, and Center for Climatic Research, University of Wisconsin—Madison, Madison, Wisconsin*

(Manuscript received 20 March 2013, in final form 2 October 2013)

### ABSTRACT

This study examines the validity of the net freshwater transport  $\Delta M_{ov}$  as a stability indicator of the Atlantic meridional overturning circulation (AMOC) in a low-resolution version of the NCAR Community Climate System Model, version 3 (CCSM3). It is shown that the sign of  $\Delta M_{ov}$  indicates the monostability or bistability of the AMOC, which is based on a hypothesis that a collapsed AMOC induces a zero net freshwater transport. In CCSM3, this hypothesis is satisfied in that the collapsed AMOC, with a nonzero strength, induces a zero net freshwater transport  $\Delta M_{ov}$  across the Atlantic basin by generating equivalent freshwater export  $M_{ovS}$  and freshwater import  $M_{ovN}$  at the southern and northern boundaries, respectively. Because of the satisfaction of the hypothesis,  $\Delta M_{ov}$  is consistent with a generalized indicator  $L$  for a slowly evolving AMOC, both of which correctly monitor the AMOC stability.

### 1. Introduction

The interaction between the freshwater cycle and the Atlantic meridional overturning circulation (AMOC) has been discussed for many years (e.g., Stommel 1961; Bryan 1986; Rahmstorf et al. 2005; Manabe and Stouffer 1988). Recent work has suggested that the key determination of the stability of the AMOC to changes in the freshwater flux depends on whether the AMOC salinifies or freshens the Atlantic (Rahmstorf 1996). A diagnostic indicator, initially the AMOC freshwater transport in the South Atlantic  $M_{ovS}$  (Rahmstorf 1996; de Vries and Weber 2005; Drijfhout et al. 2010), and later the net AMOC freshwater transport  $\Delta M_{ov}$  (Dijkstra 2007; Huisman et al. 2010; Liu and Liu 2013, hereafter LL13), was developed to assess the AMOC stability in the equilibrium state. Essentially, these indicators are based on a hypothesis derived from the box model of Rahmstorf (1996): a collapsed AMOC induces a zero net freshwater

transport ( $M_{ovS}$  or  $\Delta M_{ov} = 0$ ) because of the absence of mass transport. So for an active AMOC, the sign of  $M_{ovS}$  (or  $\Delta M_{ov}$ ) directly denotes the potential change of the AMOC-induced freshwater transport if the circulation shuts down. A positive (negative)  $M_{ovS}$  or  $\Delta M_{ov}$  indicates a potential freshwater loss (accumulation) in the Atlantic basin, which is associated with a basin-scale saltwater (freshwater)-advection feedback and then a monostable (bistable) AMOC. One critical issue is that this hypothesis from the box model is always assumed to be satisfied in all the climate models, yet previous studies have not examined the validity of this idealized hypothesis before the application of  $M_{ovS}$  ( $\Delta M_{ov}$ ) (e.g., Hawkins et al. 2011; Weaver et al. 2012; LL13). Liu et al. (2013) have shown that this idealized hypothesis may not be valid for some coupled general circulation models (CGCMs), in which the collapsed AMOC has a minor strength of 3–4 Sv (1 Sv  $\equiv 10^6 \text{ m}^3 \text{ s}^{-1}$ ) and induces a nonzero  $M_{ovS}$  ( $\Delta M_{ov}$ ) across the Atlantic basin. As a result, the sign of  $M_{ovS}$  ( $\Delta M_{ov}$ ) from an active AMOC is not reliable indicator of the AMOC stability. Therefore, it is important to verify this idealized hypothesis before using the stability indicator.

*Corresponding author address:* W. Liu, Scripps Institution of Oceanography, CASPO, 9500 Gilman Dr., La Jolla, CA, 92093.  
E-mail: wel109@ucsd.edu

In this paper, we reexamine the stability indicator of the AMOC by performing experiments using both a dipole freshwater correction to modulate the AMOC stability and a freshwater hosing to test the AMOC stability. In section 3, we demonstrate that the hypothesis is valid in the Community Climate System Model, version 3 (CCSM3), under the present-day climate, but for a very different reason from the box model. In section 4, we further show that, with the hypothesis satisfied, the conventional indicator of net freshwater transport  $\Delta M_{ov}$  becomes consistent with a generalized indicator  $L$  that applies to a slowly evolving AMOC, both correctly indicating the AMOC stability.

## 2. Model and experiments

The CGCM used in this study is the low-resolution National Center for Atmospheric Research (NCAR) CCSM3 (Yeager et al. 2006). The atmosphere component is the Community Atmospheric Model, version 3 (CAM3), with T31 spectral truncation (approximately  $3.75^\circ$  resolution). The land component is the Community Land Model, version 3 (CLM3), including dynamic vegetation. The ocean and sea ice component are the Parallel Ocean Program (POP) and the Community Sea Ice Model, version 5 (CSIM5), respectively. The ocean model adopts a nominal  $3^\circ$  horizontal resolution grid with finer resolutions toward Greenland and 25 vertical levels in the ocean known as the x3ocn grid. The sea ice model has the same horizontal resolution as the ocean.

The experimental design generally followed LL13. The control run (A) was adopted from a control run in the perpetual AD 1990 scenario, between years 780 and 980, with year 780 redented as year 0 in run A. From this control run, we applied a dipole freshwater flux correction to modulate the ocean stratification and the AMOC strength, which alters the freshwater transport and, in turn, the AMOC stability in the model (de Vries and Weber 2005; LL13). In particular, starting from year 100 in run A, four sensitivity experiments, runs B, C, D, and E, were conducted, in which an east–west dipole of anomalous freshwater flux is added and subtracted east and west of  $15^\circ\text{W}$ , respectively, over the  $17^\circ$ – $34^\circ\text{S}$  belt in the South Atlantic subtropical gyre, with an increasing strength of  $\pm 0.15$ ,  $\pm 0.25$ ,  $\pm 0.29$ , and  $\pm 0.35$  Sv (Fig. 1). The AMOC stability in the equilibrium state of runs A, B, and C was further tested with three parallel freshwater hosing experiments (runs A–H, B–H, and C–H), in which a 100-yr pulse of 1.0-Sv freshwater flux was uniformly distributed into the North Atlantic ( $50^\circ$ – $70^\circ\text{N}$ ; see Fig. 1) from year 100 in run A and from year 1100 in runs B and C. Details of the experimental designs are shown in Table 1.

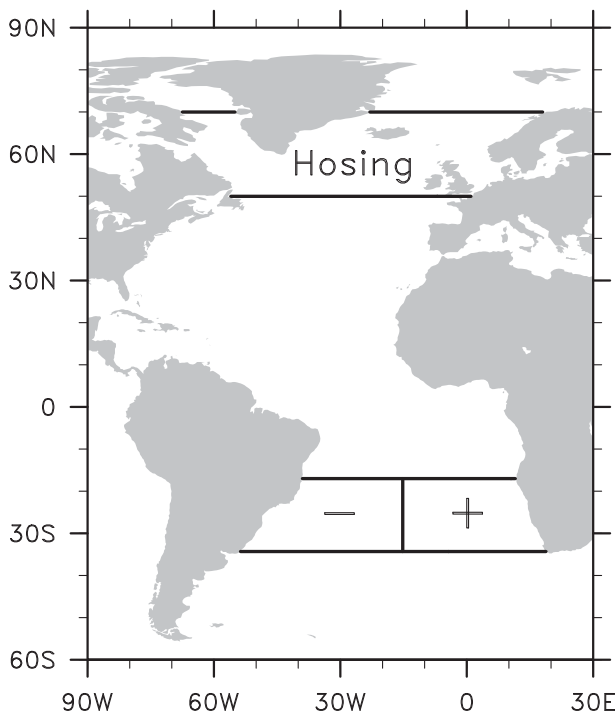


FIG. 1. The Atlantic map showing the regions of dipole perturbations and freshwater hosing. An east–west dipole of anomalous freshwater flux is added over the  $17^\circ$ – $34^\circ\text{S}$  belt in the South Atlantic subtropical gyre. The anomalous freshwater flux is negative west of  $15^\circ\text{W}$  but positive east of  $15^\circ\text{W}$  (see Table 1 for further details). The hosing region is the  $50^\circ$ – $70^\circ\text{N}$  belt within the Atlantic basin.

## 3. The generalized hypothesis

First, we examined the validity of the ideal hypothesis in CCSM3 by investigating the response of the AMOC and the AMOC-induced freshwater transport to the dipole freshwater forcing. The AMOC strength  $\psi$  is defined as the maximum in the streamfunction of the circulation below 500 m in the North Atlantic basin. The AMOC-induced freshwater transport is defined as

$$M_{ov}(\phi) = (-1/S_0) \int_{-H}^0 \langle v(\phi, z) \rangle \{ \langle s(\phi, z) \rangle - S_0 \} dz,$$

where  $v$  is the velocity normal to the section (for further details, see LL13) and  $s$  is the salinity. The vertical integration at the section is from the sea bottom  $z = -H$  to the sea surface  $z = 0$ . The angular and curly brackets indicate the along-section mean and integration, respectively. The reference salinity  $S_0 = 34.7$  psu and  $M_{ov}$  is a function of latitude  $\phi$ . Across the Atlantic basin, the AMOC induces freshwater transports either at the southern boundary ( $M_{ovS}$ ;  $\sim 34^\circ\text{S}$ ) or at the northern boundary ( $M_{ovN}$ ;  $\sim 80^\circ\text{N}$ ). As a result, the AMOC-induced freshwater transport across the Atlantic basin is

TABLE 1. The experimental design as well as the summary of the AMOC strength and stability in the experiments. Definitions of  $\psi$ ,  $\Delta M_{ov}$ , and  $L$  are described in the text. In each run,  $\psi$  is calculated from the annual mean output and shown as the last 100-yr average, and  $\Delta M_{ov}$  is calculated using monthly model output and shown as the last 100-yr average. Note here magnitudes of  $\Delta M_{ov}$  in runs D and E are very close to zero and at least one order smaller than those in runs A–C, which suggests that the collapsed AMOCs in runs D and E induce an almost divergence-free freshwater transport across the Atlantic basin (i.e.,  $\Delta M_{ov}^c \approx 0$ ). For runs A–C,  $L$  is calculated in formula of  $L = \Delta M_{ov} / (\overline{\psi^a} - \overline{\psi^c})$ , where  $\overline{\psi^a}$  is taken as the value of  $\psi$  in each run and  $\overline{\psi^c}$  is taken as the averaged value of  $\psi$  between runs D and E (i.e.,  $\overline{\psi^c} = 7.0$  Sv). Based on both  $\Delta M_{ov}$  and  $L$ , the AMOCs are monostable in runs A and B but bistable in run C.

| Run | Dipole (Sv) | Hosing (Sv) | Period (yr) | $\psi$ (Sv) | $\Delta M_{ov}$ (Sv) | $L$ ( $\times 10^3$ ) | AMOC stability |
|-----|-------------|-------------|-------------|-------------|----------------------|-----------------------|----------------|
| A   | 0           | 0           | 0–200       | 15.0        | 0.112                | 14.3                  | Monostable     |
| B   | $\pm 0.15$  | 0           | 100–1100    | 14.0        | 0.010                | 1.4                   | Monostable     |
| C   | $\pm 0.25$  | 0           | 100–1100    | 13.5        | –0.038               | –5.8                  | Bistable       |
| D   | $\pm 0.29$  | 0           | 100–1000    | 7.3         | –0.001               | —                     | —              |
| E   | $\pm 0.35$  | 0           | 100–800     | 6.7         | –0.001               | —                     | —              |
| A-H | 0           | 1.0         | 100–900     | 16.4        | 0.119                | —                     | —              |
| B-H | $\pm 0.15$  | 1.0         | 1100–2300   | 14.9        | 0.012                | —                     | —              |
| C-H | $\pm 0.25$  | 1.0         | 1100–2700   | 8.2         | –0.015               | —                     | —              |

defined as  $\Delta M_{ov} = M_{ovS} - M_{ovN}$ . Figure 2 shows that as the freshwater forcing intensifies, the strength of the AMOC generally decreases over the first 400 hundred years, with the decreasing magnitude roughly proportional to the magnitude of the freshwater forcing. This quasilinear response, however, changes dramatically at the final equilibrium state. The AMOC tends to recover to around 14 Sv in the cases of weak dipole forcing (runs B and C) but collapses to approximately 7 Sv in the cases of strong dipole forcing (runs D and E). This response is consistent with results shown by Cimadoribus et al. (2012). In run D, the AMOC weakens gradually, reaching a quasi-steady collapsed state of 7.3 Sv after 700 yr. In run E, the AMOC strengthens in the initial 100 yr and then rapidly weakens (within 200 yr) to a steady collapsed state of 6.7 Sv at year 400 (Fig. 2a). It is worth noting that as the AMOC collapses in runs D and E, the freshwater export in the south,  $M_{ovS}$ , approaches the freshwater import from the north,  $M_{ovN}$  (Fig. 2c), such that the net freshwater transport across the Atlantic basin (or transport divergence) almost vanishes ( $\Delta M_{ov} \approx 0$ ) in the collapsed state (Fig. 2b). This demonstrates that the hypothesis is indeed valid in CCSM3, but for a very different reason from the box model. In the box model, a zero freshwater transport across the Atlantic basin results from a zero strength of the AMOC. In contrast, CCSM3 produces a collapsed AMOC with a nonzero strength. However, this collapsed AMOC can still induce a zero net freshwater transport by generating equal and compensating freshwater export and import across the southern and northern boundaries, respectively. Therefore, we should modify the original hypothesis to a generalized hypothesis simply as follows: a collapsed AMOC induces a zero net freshwater transport ( $\Delta M_{ov} = 0$ ).

#### 4. Testing the AMOC stability

Since the hypothesis is valid, the sign of  $\Delta M_{ov}$  for an active AMOC should still be valid to indicate the AMOC stability. In particular, a positive  $\Delta M_{ov}$  (freshwater convergence) indicates a monostable AMOC, because an AMOC shutdown will tend to salinify the Atlantic basin, leading to an AMOC recovery. On the other hand, a negative  $\Delta M_{ov}$  (freshwater divergence) indicates a bistable AMOC, in that an AMOC shutdown will induce a freshwater accumulation in the basin, which helps to suppress deep convection in the North Atlantic and therefore maintain a stable shutdown state. This could be tested in runs A, B, and C. As seen from Fig. 2, the AMOC is active ( $\sim 13$ – $15$  Sv) in the equilibria of runs A–C. However, runs A and B have a freshwater convergence ( $\Delta M_{ov} > 0$ ) while run C has a freshwater divergence ( $\Delta M_{ov} < 0$ ). Therefore, the stability indicator suggests a monostable AMOC in runs A and B, but a bistable AMOC in run C.

The stability of the AMOC in runs A, B, and C was indeed confirmed explicitly in three parallel hosing experiments (runs A-H, B-H, and C-H). In these hosing experiments, a strong pulse of freshwater perturbation was imposed over the North Atlantic ( $50^\circ$ – $70^\circ$ N) where the deep water forms. As shown in Fig. 3, the strong freshwater discharge in the North Atlantic shuts down the AMOCs in all three cases during the 100-yr hosing period. However, in runs A-H and B-H, after the termination of the hosing, excessive salt accumulates in the basin and the associated salinity advection feedback reignites deep convection in the North Atlantic, leading to a resumption of the AMOC. As a result, not only the AMOC itself but also the AMOC-induced freshwater transports ( $M_{ovS}$ ,  $M_{ovN}$ , and  $\Delta M_{ov}$ ) eventually recover in runs A-H and B-H (Figs. 3a–d). All these demonstrate that the AMOCs are monostable in runs A and B. In

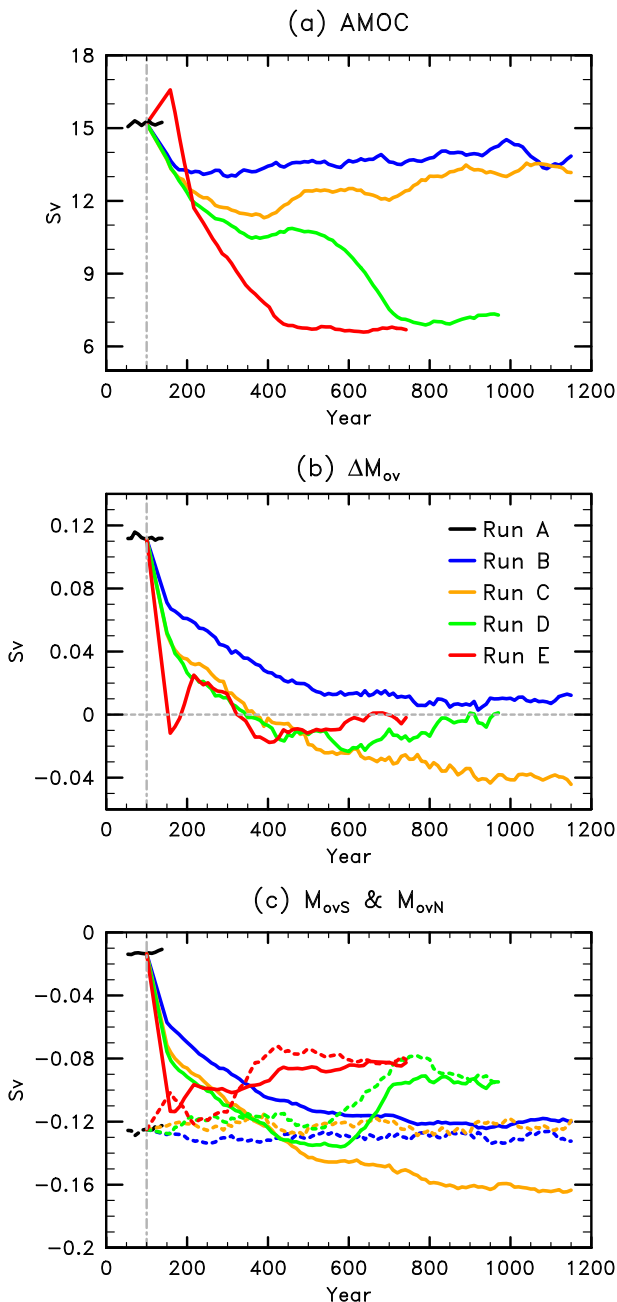


FIG. 2. Time evolution of (a) the AMOC strength  $\psi$ , (b) the net freshwater transport in the Atlantic basin  $\Delta M_{ov}$  as induced by the AMOC, and (c) the overturning freshwater transports across the southern and northern boundaries, which are,  $M_{ovS}$  (solid lines) and  $M_{ovN}$  (dashed lines) respectively, in runs A (black), B (blue), C (orange), D (green), and E (red). The AMOC strength  $\psi$  is calculated from the annual mean output and shown as a decadal mean, with 100-yr running average. Note that  $M_{ovS}$ ,  $M_{ovN}$ , and  $\Delta M_{ov}$  are calculated from the monthly output and shown in decadal means, with 100-yr running average. The vertical dashed-dotted line (gray) denotes the time when the dipole of anomalous freshwater flux is added in the South Atlantic. The results of runs A and C are redrawn from LL13.

contrast, in run C-H, excessive freshwater accumulates in the basin, inhibiting the recovery of the AMOC. Therefore, the AMOC remains in its stable collapsed state after the termination of the hosing (Fig. 3e). Meanwhile,  $M_{ovS}$  approaches  $M_{ovN}$  such that  $\Delta M_{ov}$  becomes approximately nondivergent (Fig. 3f). All these features suggest a bistable AMOC in run C, with the strong hosing perturbation triggering the AMOC switching from an active state to a collapsed state.

Collecting the equilibrium values of  $\psi$  and  $\Delta M_{ov}$  from all the runs allows us to plot two stability diagrams:  $\psi$  versus the strength of the dipole forcing (Fig. 4a) and  $\psi$  versus  $\Delta M_{ov}$  (Fig. 4b). Figure 4a shows two branches of the AMOC: the active branch with a volume transport of  $\psi \sim 13.5\text{--}15.0$  Sv, and the collapsed branch with  $\psi \sim 6.7\text{--}7.3$  Sv. A strong freshwater perturbation can trigger a switch between two branches when the AMOC resides in a bistable regime. Also, it was shown that the dipole freshwater forcing can modulate the AMOC stability. The AMOC in run A is in the monostable regime ( $\Delta M_{ov} > 0$ ). With an increasing dipole forcing,  $\Delta M_{ov}$  decreases and becomes negative, so that the AMOC stability shifts from a monostable regime to a bistable regime (Fig. 4b). When the dipole forcing is strong enough (equal and greater than  $\pm 0.29$  Sv for runs D and E in this study), it can also trigger a change of the AMOC, from the active branch to the collapsed branch.

## 5. The consistency between the indicators $\Delta M_{ov}$ and $L$

A generalized indicator of the AMOC stability  $L$  was introduced by Liu et al. (2013). This indicator has been formulated for  $L = \partial \overline{\Delta M_{ov}} / \partial \overline{\psi}$ , where  $\overline{\psi}$  and  $\overline{\Delta M_{ov}}$  are the strength and net freshwater transport of the AMOC in a quasi-equilibrium state (the overbar denotes temporal averaging over a sufficient time to achieve an quasi-equilibrium value). Nevertheless  $L$  denotes a relative freshwater transport, that is, the change of  $\Delta M_{ov}$  when the AMOC transits from one (quasi-)equilibrium to another (quasi-)equilibrium, so that the default hypothesis of  $\Delta M_{ov} = 0$  (for a collapsed AMOC) is no longer needed. Generally speaking,  $\Delta M_{ov}$  and  $L$  have different criteria for the AMOC stability (see Liu et al. 2013), and they can only become consistent with each other when the default hypothesis for  $\Delta M_{ov}$  is satisfied, such as the case in this study. The reason is that, when the AMOC transits from an active state to a collapsed state,  $L$  can be calculated as  $L = (\overline{\Delta M_{ov}^a} - \overline{\Delta M_{ov}^c}) / (\overline{\psi^a} - \overline{\psi^c})$ , where the overbar refers to the value in the quasi-equilibrium and the superscripts  $a$  and  $c$  refer to active and collapsed states. Because of the satisfaction of the idealized hypothesis,  $\overline{\Delta M_{ov}^c} = 0$ , the generalized indicator becomes

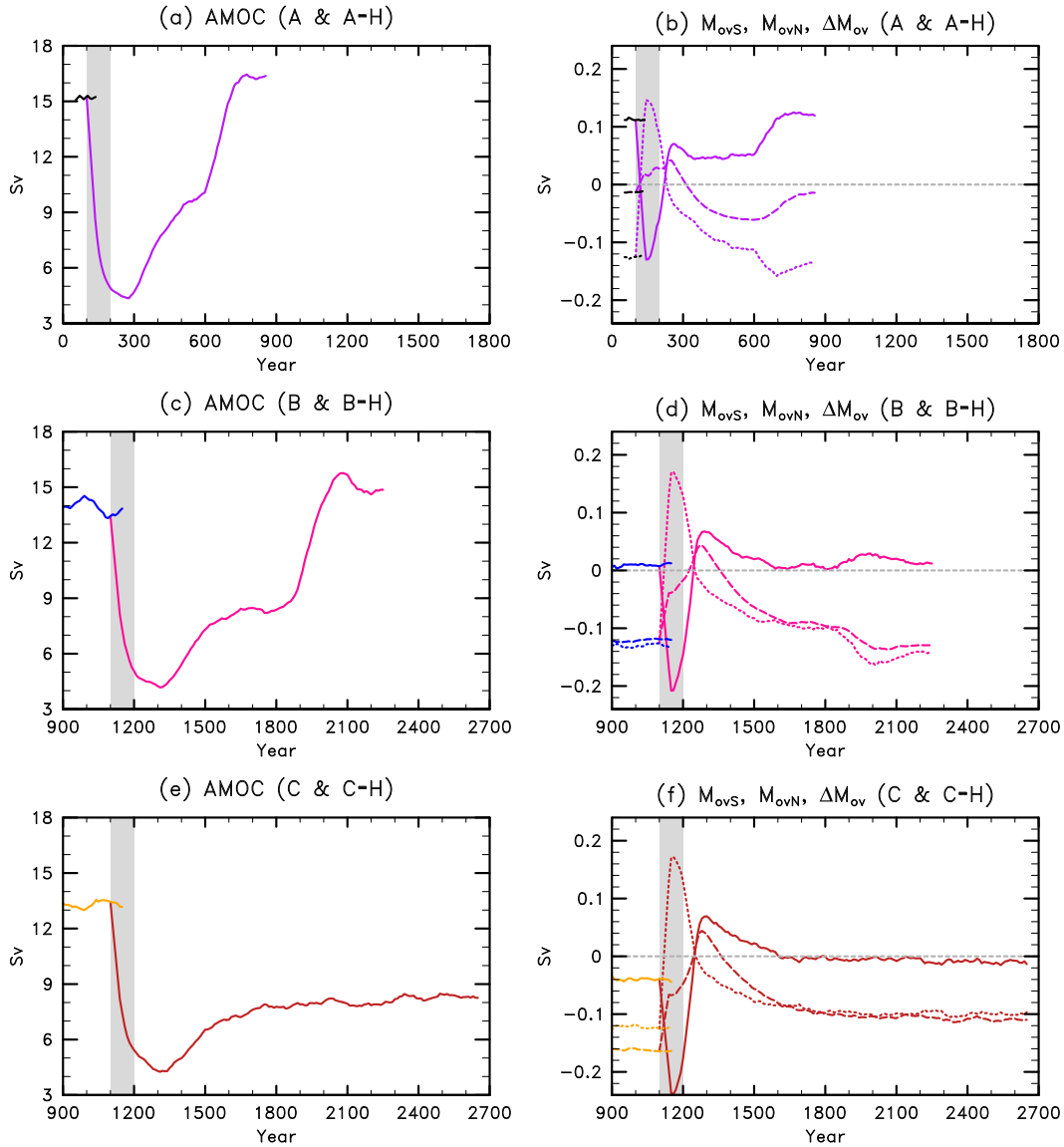


FIG. 3. Time evolution of (left) the AMOC strength  $\psi$  and (right)  $M_{ovS}$  (dashed line),  $M_{ovN}$  (dotted line), and  $\Delta M_{ov}$  (solid line) in (a) runs A (black) and A-H (purple), (b) runs B (blue) and B-H (deep pink), and (c) runs C (orange) and C-H (brown). The AMOC strength  $\psi$  is calculated from the annual mean output and shown as a decadal mean, with 100-yr running average;  $M_{ovS}$ ,  $M_{ovN}$ , and  $\Delta M_{ov}$  are calculated from the monthly output and shown in decadal means, with 100-yr running average. The gray shading denotes a 100-yr hosing period. Values of  $\psi$  in runs A, A-H, C, and C-H are redrawn from LL13.

$L = \overline{\Delta M_{ov}^a} / (\overline{\psi^a} - \overline{\psi^c}) = \Delta M_{ov} / (\overline{\psi^a} - \overline{\psi^c})$ , and it always shares the same sign with  $\Delta M_{ov}$  since  $\overline{\psi^a} - \overline{\psi^c} > 0$ . Therefore,  $L$  is positive in runs A and B, representing a negative feedback between  $\psi$  and  $\Delta M_{ov}$  and thus a monostable AMOC; in contrast,  $L$  is negative in run C, which represents a positive feedback and a bistable AMOC (Table 1). In addition, the absolute value of  $L$  is proportional to the strength of the feedback. So, comparing with run B, a larger  $L$  in run A (Table 1) indicates a stronger negative feedback between  $\psi$  and  $\Delta M_{ov}$  and

thus an AMOC with stronger stability. This conclusion was verified by the hosing experiments, in which the AMOC in run A-H has a much quicker recovery (300 yr earlier) than run B after the termination of the freshwater perturbation (Fig. 3).

### 6. Conclusions

In this study, we reexamined the stability indicator of the AMOC  $\Delta M_{ov}$  in CCSM3. As derived from the box

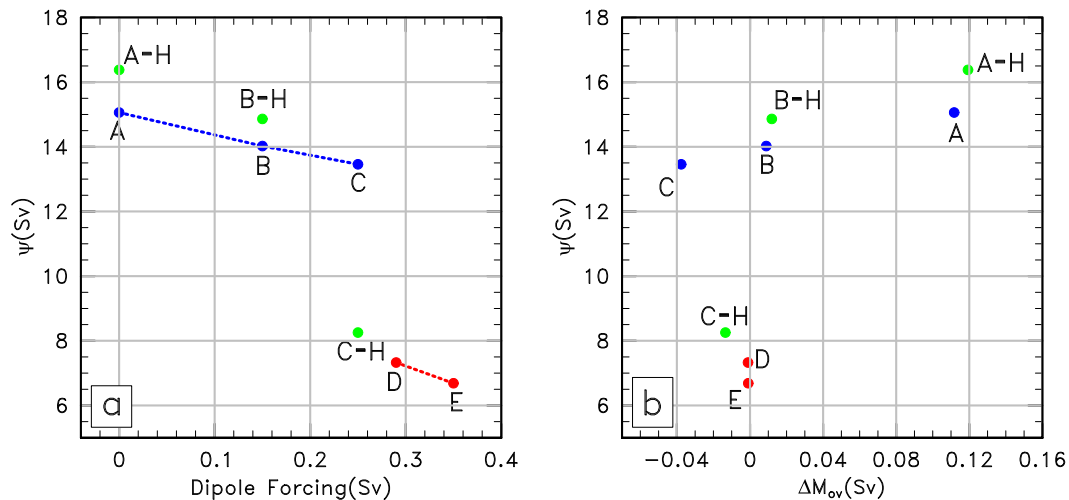


FIG. 4. The AMOC stability diagrams (a)  $\psi$  vs the strength of the dipole forcing and (b)  $\psi$  vs  $\Delta M_{ov}$ ;  $\psi$  is calculated from the annual mean output and shown as the last 100-yr average, and  $\Delta M_{ov}$  is calculated from monthly model output and shown as the last 100-yr average. Results of  $\psi$  and  $\Delta M_{ov}$  are divided into three groups and dotted by different colors: the active AMOC group (runs A–C; blue), the collapsed AMOC group (runs D and E; red), and the hosing group (runs A–H, B–H, and C–H; green). In (a), auxiliary dotted lines are added to manifest the active and collapsed branches of the AMOC, which do not represent a continuous AMOC response for the dipole forcing.

model, the key to the validity of  $\Delta M_{ov}$  is a hypothesis (i.e., a zero AMOC-induced freshwater transport across the Atlantic basin for a collapsed circulation). We found that this hypothesis is still achieved in CCSM3, but for a different reason: the collapsed AMOC has a nonzero mass transport as well as nonzero freshwater transports  $M_{ovS}$  and  $M_{ovN}$ , but a zero net freshwater transport  $\Delta M_{ov}$  because of the equal and compensating  $M_{ovS}$  and  $M_{ovN}$  at the southern and northern boundaries. Therefore, the hypothesis should be changed to only indicate  $\Delta M_{ov} = 0$ , not necessarily an AMOC strength of zero. The satisfaction of the hypothesis not only ensures the validity of  $\Delta M_{ov}$  as an indicator but also offers a consistent assessment between  $\Delta M_{ov}$  and a generalized indicator  $L$ . As such, a positive  $\Delta M_{ov}$  or  $L$  indicates a monostable AMOC whereas a negative  $\Delta M_{ov}$  or  $L$  indicates a bistable AMOC.

These results also allow us to make some comments on how one might determine the AMOC stability from observations. The hypothesis can be easily tested in numerical models but not in observations, because 1) current observations of  $M_{ovS}$  and  $M_{ovN}$  are for an active AMOC and 2) it is difficult to estimate either  $M_{ovS}$  or  $M_{ovN}$  for a historically collapsed AMOC (such as the AMOC during the Heinrich 1 event) from scattered proxy records. Therefore, currently, we can only assume that the model simulation is consistent with observations (i.e.,  $\Delta M_{ov}$  will equal to or be close to zero if the real AMOC collapses) and then estimate the stability of the current AMOC. Meanwhile, it is worth noting that

$L$  may be a desirable indicator for observations since 1)  $L$  is independent of the hypothesis and 2) the current AMOC is slowly evolving under various forcings ( $CO_2$  forcing, aerosol forcing, etc.). Therefore, we need long-term observations of the AMOC strength and both the northern and southern boundaries of the AMOC freshwater transport for an estimation of  $L$ .

**Acknowledgments.** This study is supported by the Priority Academic Program Development of Jiangsu Higher Education Institutions (PAPD). The work is also supported by NSF and NSFC 41130105.

## REFERENCES

- Bryan, F., 1986: High-latitude salinity effects and interhemispheric thermohaline circulations. *Nature*, **323**, 301–304.
- Cimatoribus, A. A., S. S. Drijfhout, M. den Toom, and H. A. Dijkstra, 2012: Sensitivity of the Atlantic meridional overturning circulation to South Atlantic freshwater anomalies. *Climate Dyn.*, **39**, 2291–2306, doi:10.1007/s00382-012-1292-5.
- de Vries, P., and S. L. Weber, 2005: The Atlantic freshwater budget as a diagnostic for the existence of a stable shut down of the meridional overturning circulation. *Geophys. Res. Lett.*, **32**, L09606, doi:10.1029/2004GL021450.
- Dijkstra, H. A., 2007: Characterization of the multiple equilibria regime in a global ocean model. *Tellus*, **59A**, 695–705.
- Drijfhout, S. S., S. L. Weber, and E. van der Swaluw, 2010: The stability of the MOC as diagnosed from model projections for pre-industrial, present and future climates. *Climate Dyn.*, **37**, 1575–1586, doi:10.1007/s00382-010-0930-z.
- Hawkins, E., R. S. Smith, L. C. Allison, J. M. Gregory, T. J. Woollings, H. Pohlmann, and B. de Cuevas, 2011: Bistability of the Atlantic overturning circulation in a global climate

- model and links to ocean freshwater transport. *Geophys. Res. Lett.*, **38**, L10605, doi:10.1029/2011GL047208.
- Huisman, S. E., M. Den Toom, H. A. Dijkstra, and S. S. Drijfhout, 2010: An indicator of the multiple equilibria regime of the Atlantic meridional overturning circulation. *J. Phys. Oceanogr.*, **40**, 551–567.
- Liu, W., and Z. Liu, 2013: A diagnostic indicator of the stability of the Atlantic meridional overturning circulation in CCSM3. *J. Climate*, **26**, 1926–1938.
- , —, and A. Hu, 2013: The stability of an evolving Atlantic meridional overturning circulation. *Geophys. Res. Lett.*, **40**, 1562–1568, doi:10.1002/grl.50365.
- Manabe, S., and R. J. Stouffer, 1988: Two stable equilibria of a coupled ocean–atmosphere model. *J. Climate*, **1**, 841–866.
- Rahmstorf, S., 1996: On the freshwater forcing and transport of the Atlantic thermohaline circulation. *Climate Dyn.*, **12**, 799–811.
- , and Coauthors, 2005: Thermohaline circulation hysteresis: A model intercomparison. *Geophys. Res. Lett.*, **32**, L23605, doi:10.1029/2005GL023655.
- Stommel, H., 1961: Thermohaline convection with two stable regimes of flow. *Tellus*, **2**, 244–230.
- Weaver, A. J., and Coauthors, 2012: Stability of the Atlantic meridional overturning circulation: A model intercomparison. *Geophys. Res. Lett.*, **39**, L20709, doi:10.1029/2012GL053763.
- Yeager, S. G., C. A. Shields, W. G. Large, and J. J. Hack, 2006: The low-resolution CCSM3. *J. Climate*, **19**, 2545–2566.